

Aeroelastic Investigation of Different Deck Sections for Suspension Bridges by Numerical Analysis

Ahmed Abdel-Aziz, Walid A. Attia

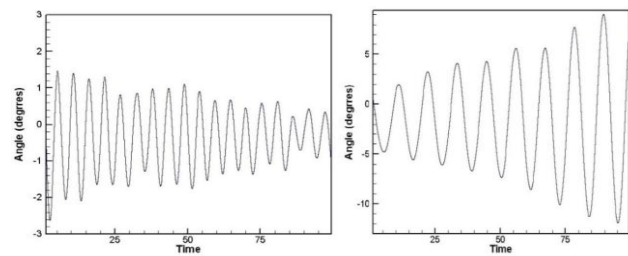
Abstract— Computational fluid dynamics (CFD) simulations appear to be a strong competitor to wind tunnel tests which are expensive, require a scale model and a time consuming tool in designing bridges, therefore there is a strong claim to replace them with CFD. Analyses are carried out for four deck cross sections by secondary development of CFD software Ansys Fluent, establishing a dimensional bending and torsional fluid-structure interaction (FSI) numerical model to calculate the flutter critical wind speed. Steady and unsteady simulations have been computed in order to judge the feasibility of CFD simulations in the early stage design of long span bridges. Additionally, a realizable (κ - ϵ) model with enhanced wall treatment and a (κ - ω SST) turbulence model have been considered to verify their performance in bridge aerodynamics problems. It has been found that static aerodynamic coefficients have been correctly modeled using a steady simulation, while the flutter critical wind speed is judged from the time history of unsteady simulations for stationary deck sections. The validity of the simulation method was verified by comparison of the simulation results with the work done by other researchers.

Index Terms— Bridge aeroelasticity, Computational fluid dynamics, Critical flutter wind speed, Suspension bridges

I. INTRODUCTION

Wind load is one of the most important design loads in civil engineering structures, especially for long span bridges with low damping and high flexibility. Deck sections of long span bridges are one type of bluff bodies that are usually elongated with sharp corners that make the flow around them to cause aerodynamic instabilities. Such instabilities may cause serious catastrophic structural failure such as, the Old Tacoma Narrows Bridge collapse in 1940. Suspension bridges not only must be designed to support static wind forces like lift, drag and moment created by the mean wind, but also the dynamic loads created by an interaction between the wind forces and structural motions which is known as aeroelasticity. Deck models are used in wind tunnel tests to obtain aerodynamic and aeroelastic information. However, with computer technology and CFD evolution, a lot of these models can also be analyzed by numerical simulations. Flutter occurs due to a structure and wind interaction where the wind speed has passed the critical speed of flutter and negative damping develops [1]. If a structure is experiencing oscillation a positive damping will slowly decrease the amplitude of displacement, on the other hand flutter increases

the amplitude of the oscillation as time continues [2]. Fig. 1 shows a sinusoidal representation of both positive and negative damping phenomena.



(a) Positive damping (b) Negative damping

Fig. 1 Example of positive and negative damping [3]

Galloping, vortex shedding vibrations, and flutter are the most aeroelastic phenomena that can be seen in long span suspension bridges. Only the last phenomenon will be studied in the present work and will be focused on producing reliable results over a range of different bridge deck sections, establishing a dimensional bending and torsional fluid-structure interaction numerical model and a finite element solver to calculate the critical wind speed of flutter for different deck sections and determining whether the computational method can lead to a reduction in the number of expensive physical model tests.

II. METHODOLOGY

A. Numerical Simulation Principle

The structure is regarded as a mass, spring and damping system. A schematic diagram of numerical simulation is shown in Fig.2. Fluid control equations for incompressible flow are given in Equations (1) and (2) which represent the continuity and the Navier-Stokes equation respectively. The first step to ascertain the aerodynamic response of the considered bridge deck types is computation of the aerodynamic force coefficients (C_d, C_l, C_m). After getting these coefficients, forces (F_D, F_L, M) can be easily calculated by Equations (3), (4) and (5) [4]. Fig.3 shows criteria for the aerodynamic forces and moment. Equations (6) and (7) are the governing structural equations for the heaving and torsional mode [2].

$$\nabla \cdot V = 0 \quad \text{[Eqn. 1]}$$

$$\frac{\partial v}{\partial t} + (V \cdot \nabla)V = -\frac{1}{\rho} \nabla p + \mu \nabla^2 V \quad \text{[Eqn. 2]}$$

$$F_D = 0.5 \rho U^2 B C_d \quad \text{[Eqn. 3]}$$

$$F_L = 0.5 \rho U^2 B C_l \quad \text{[Eqn. 4]}$$

$$M = 0.5 \rho U^2 B^2 C_m \quad \text{[Eqn. 5]}$$

$$m \ddot{h}(t) + C_h \dot{h}(t) + K_h h(t) = F_L(t) \quad \text{[Eqn. 6]}$$

$$I \ddot{\alpha}(t) + C_\alpha \dot{\alpha}(t) + K_\alpha \alpha(t) = M(t) \quad \text{[Eqn. 7]}$$

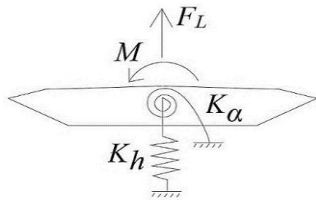


Fig. 2 Schematic diagram of numerical simulation.

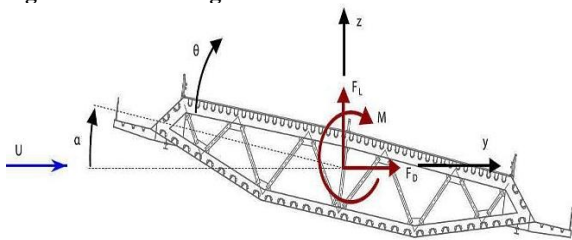


Fig. 3 Sign criteria for the aerodynamic Forces [4].

Where:

V, p and t: Velocity, pressure, time respectively.

ρ : Air density.

μ : Air dynamic viscosity.

F_D, F_L, M : Drag force, lift force, and moment respectively.

C_d, C_l, C_m : Coefficients of drag force, lift force, and moment respectively.

U: Reference velocity.

B: Bridge width.

m: Deck mass per unit length.

I: Mass moment of inertia about shear center per unit length.

C_h, C_α : Structural damping coefficients.

K_h, K_α : Translational and rotational spring stiffness.

$\ddot{h}(t), \dot{h}(t), h(t)$: Instantaneous bending acceleration, velocity and displacement respectively.

$\ddot{\alpha}(t), \dot{\alpha}(t), \alpha(t)$: Instantaneous torsional acceleration, velocity and displacement respectively.

The critical velocity for bridges is calculated using FSI. The aeroelastic stability is observed from the free motion of the bridge deck for various wind speeds. The procedure of FSI simulation in every wind speed is shown in Fig.4.

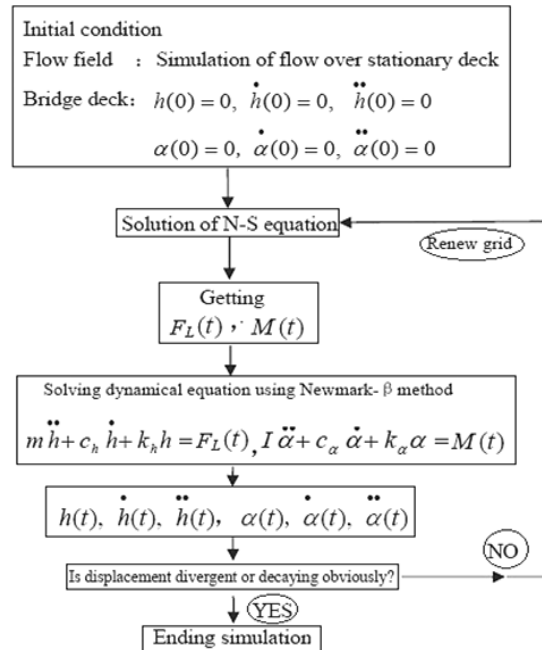


Fig. 4 Procedure of FSI in every wind speed [5]

Before calculating the time step, the preliminary value of bending and torsional acceleration, velocity, and displacement are set to be zero [5, 6]. For every time step the pressure and velocity are computed around the bridge deck for the given position by solving the continuity and Navier-Stokes equations as Equations (1) and (2). Then the aerodynamic force coefficients acting on the bridge deck are calculated by using Equations (4) and (5). This can be done by Fluent [7, 8].

Lift pressure force and moment are represented by the force in y-direction and the force that causes rotation respectively. Lift force is applied at the center of gravity and the moment is applied at the shear center, then the lift and moment are extracted into structural dynamic Equations (6) and (7). Then they are solved by using The Newmark- β method to get the displacements for the heave and pitch. These displacements are applied in a rigid body fashion and the grid is updated. The velocity of the grid is applied from one time step to the next one by dividing the time step size in different positions. This process is repeated for several time steps. Then the velocity of the grid is extracted in the Navier stokes equation to account and simulate deck movement by a dynamic mesh technique. This can be done by secondary development of Ansys Fluent which program code is embedded in it by the user defined function (UDF) Simulations of wind speed ends if the displacement divergent or decaying is observed. The critical velocity of flutter is found by plotting the time history of the structure motion induced response.

B. Numerical Simulation Model

Four bridge deck sections were studied numerically using a CFD software in order to create an empirical reference set for numerical investigations. Among these deck sections is deck section (1) which is the same section as that of the Great Belt East Bridge in Denmark .Table 1 shows all full scale parameters of it. All deck sections have the same width of 31m and the same height of 4 m. Fig.5 shows the geometric definitions of them. CFD methodology for both steady and unsteady simulations is shown in Fig.6. 2D analyzed sections have been modeled by the incompressible turbulence of the Navier-Stokes equations. There are two different equations of Reynolds Averaged Navier-Stokes (RANS) that have been employed in the simulations: realizable (κ - ϵ) model with enhanced wall treatment and (κ - ω SST) Shear-Stress Transport.

At the inlet and outlet boundaries Dirichlet conditions have been committed; however at deck sections surface no-slip conditions have been imposed. The turbulent flow characteristics have been defined with respect to the intensity and viscosity ratio. For the pressure-velocity a coupling implicit scheme for second-order and PISO algorithm are used. It is found that the PISO scheme for pressure-velocity coupling provides faster convergence for transient flow than the standard SIMPLE approach [7, 9].

The time step was equal to 0.001 in the transient state simulations for (t^*) equal to 60 seconds and the number of iterations per each time step was 10. Unsteady simulations continued until a periodic behavior was reached. Computations have been carried out on core i7, 2.10 GHz, and physical memory 8.00 GB.

Table 1 Full scale properties of the deck section (1) [1]

Parameters	Units	Values
Natural vertical frequency (f_v)	Hz	0.097
Natural torsional frequency (f_t)	Hz	0.27
Mass per unit length (m)	kg/m	23 687
Mass moment of inertia about shear center per unit length (I)	Kg.m ² /m	2.501 x10 ⁶
Equivalent spring stiffness for vertical bending mode per unit length (K_b)	Kg/m ²	878.506
Equivalent spring stiffness for torsional mode per unit length (K_α)	Kg.m/m	7.194 x10 ⁵

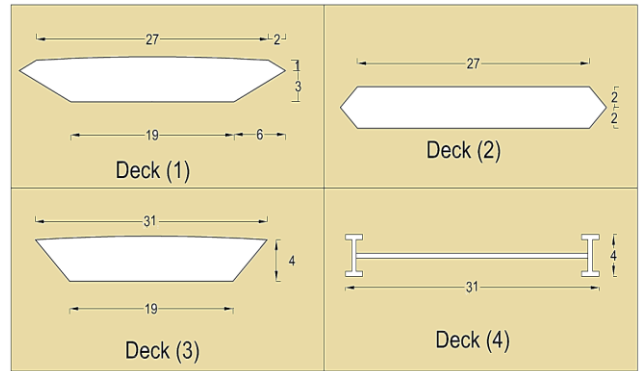


Fig. 5 Geometric definition of the deck cross sections

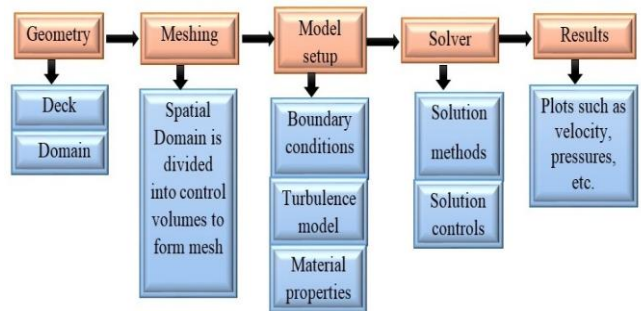


Fig. 6 Flow chart for "CFD methodology" over bridge deck

The height of the fluid domain is 10 B and the length is 16 B where (B) is the deck width. Rigid mesh grid is used in the inner region while stationary mesh grid is used in the outer region. Dynamic mesh grid is between the rigid mesh and stationary mesh. The width and height of the rigid mesh are about two times and one times the width of the deck section respectively. Both the width and height of the dynamic mesh grid are about six times the width of the deck section. Fig.7 shows the domain regions and dimensions.

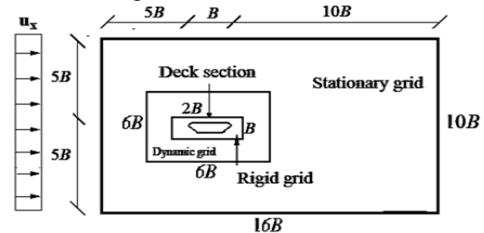


Fig. 7 Domain regions and dimensions [5].

When the deck section vibrates, the rigid mesh grid follows the deck section synchronously. The static grid stays stationary while the shape and dimension of the dynamic mesh changes constantly. In the region which is far away from the deck section, the size of the mesh grid is big. On the contrary, in the region which is near the deck section is small.

The mesh information and size are defined by the number of cells, nodes, and faces. Fig.8 and Table 2 show the

definition of them. The whole numerical grids of the four deck sections are shown in Fig.9.

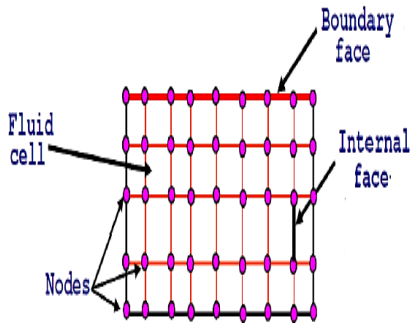
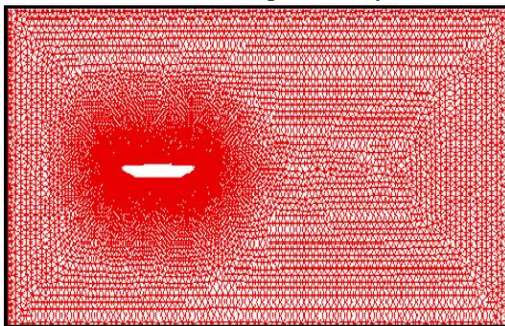


Fig. 8 Definition of cells, nodes, and face [7]

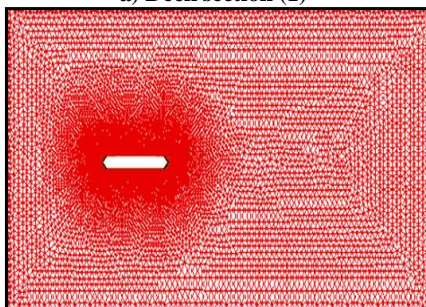
Table 2 Mesh information for studied deck sections (CFD-Model)

Deck No.	Cells	Nodes	Faces
1	97360	53996	151356
2	95212	47969	143181
3	226424	113734	340158
4	155062	78274	233336

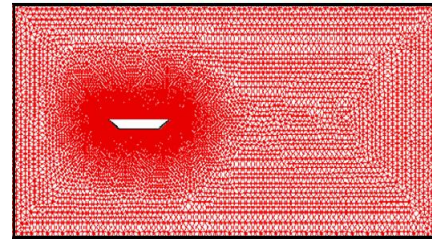
The flow runs from the left to the right. The left side is considered as the inflow boundary specified with the velocity inlet. On the other right side there is an exit boundary specified with pressure outlet equal to zero. The upper and lower sides are specified as symmetrical. The deck edges are considered as a wall with no-slip boundary conditions.



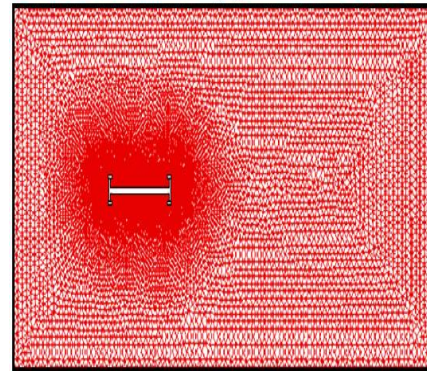
a) Deck section (1)



b) Deck section (2)



c) Deck section (3)



d) Deck section (4)

Fig. 9 Whole mesh for different deck sections

III. SIMULATION RESULTS

A. Steady Aerodynamic Force Coefficients

In order to validate the cross-sectional geometry adopted for suspension bridges, the finite volume grid and the 2D approach in the CFD analysis of the deck are used. Static aerodynamic coefficients have been computed assuming steady state for each deck. The aerodynamic coefficients have been computed for Reynolds number equal to 2.5×10^5 based on the deck width with different angles of attack in the range of -10° to 10° with step 1° .

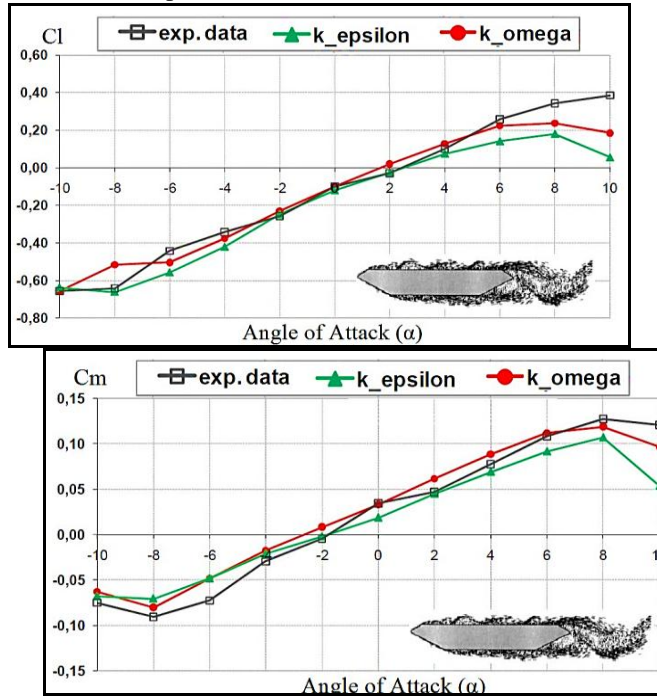
Two different Reynolds averaged turbulence models have been considered:

- 1- Realizable (k- ϵ) with enhanced wall treatment.
- 2-Shear-Stress Transport ($k-\omega$ SST).

In each case of studied turbulence models a second order scheme was used. The number of chosen iterations was 2000 in steady state simulations.

In Fig.10 the computed static aerodynamic force coefficients are presented along with the experimental results obtained by Félix [4] for the same Reynolds number and section (deck section 1).The computational results are very close to that obtained from wind tunnel tests. There are no significant differences in the results offered by (k- ϵ) and (k- ω SST) turbulence models. In general the static aerodynamic coefficients computed with (k- ϵ) turbulence model are slightly lower than those obtained using (k- ω SST) turbulence model. From Fig.10 it can be concluded that mean force

coefficients are in good agreement with the experimental data of the deck section (1).



(a) Lift coefficient (C_l) (b) Moment coefficient (C_m)

Fig. 10 Aerodynamic coefficients of deck section (1) for ($Re=2.5 \times 10^5$).

B. Unsteady Time History of Aerodynamic Coefficients

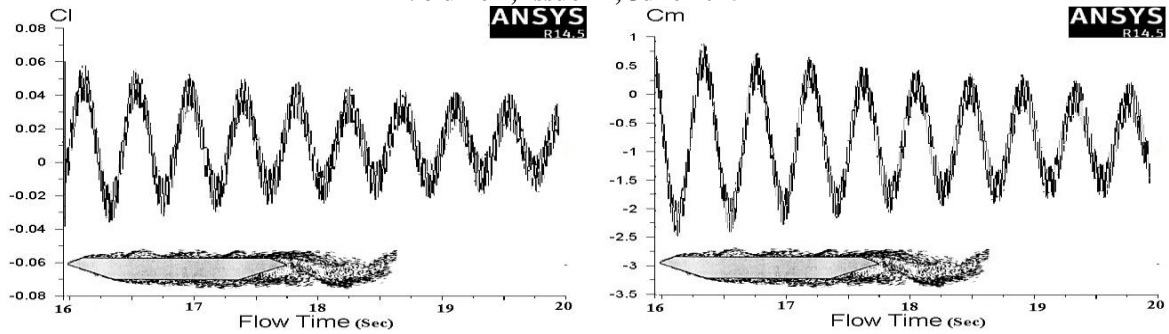
To find the critical wind speed of flutter for each deck cross section, time history analysis for aerodynamic coefficients and vibrating motion should be applied by increasing the inlet velocity incrementally in different runs. When the aerodynamic coefficients and motion amplitude started to grow (negative damping), the critical velocity was found. From Fig.s 11 and 12 for deck section (1) it can be seen that:

- When wind speed equals 68 m/sec, lift and moment coefficients decrease with the increase of time. This illustrates that the total damping of the model is positive.
- When wind speed equals 69 m/sec, lift and moment coefficients remain almost the same.
- When wind speed reaches 70 m/sec, lift and moment coefficients increase with the increase of time. This illustrates that the total damping of the model changes from positive to negative. So flutter critical wind speed equals 70 m/sec.
- When flutter occurs, the torsional vibration frequency equals 0.2 Hz. Comparing this frequency with (f_v, f_t) shown in Table 1, flutter style for deck section (1) is bending torsional coupled flutter.

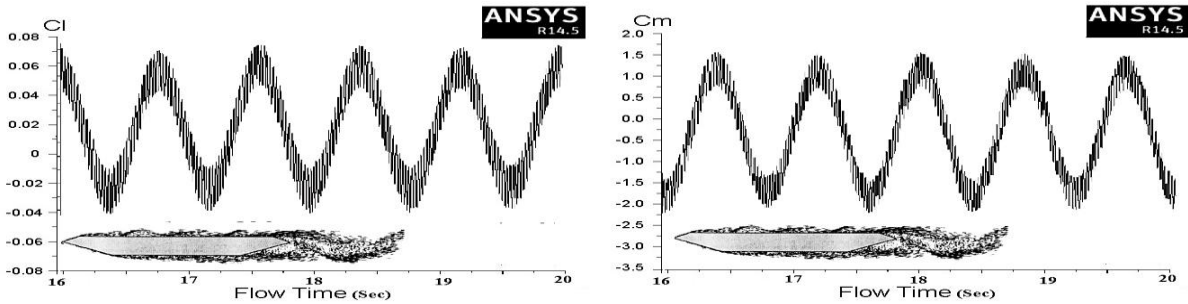
These previous investigations were repeated for deck sections 2, 3 and 4 until negative damping occurred in each deck section. Table 3 and Fig.s 13, 14 and 15 show how critical wind speed of flutter is obtained from time history of unsteady simulations for different deck sections.

Table 3 Getting flutter critical wind speed from time histories of unsteady simulations.

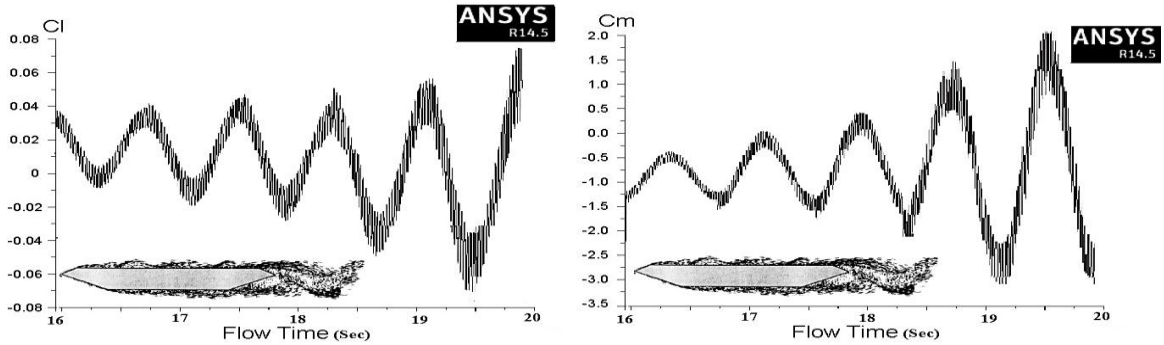
Deck cross section No.	1	2	3	4
The force acting on the deck gradually decreased at inlet velocity equal (positive damping)	68 m/sec	63 m/sec	60 m/sec	25 m/sec
The force acting on the deck gradually increased at inlet velocity equal (negative damping)	70 m/sec	64 m/sec	61 m/sec	26 m/sec
<i>So Critical wind speed of flutter equal</i>				



a) V= 68 m/sec

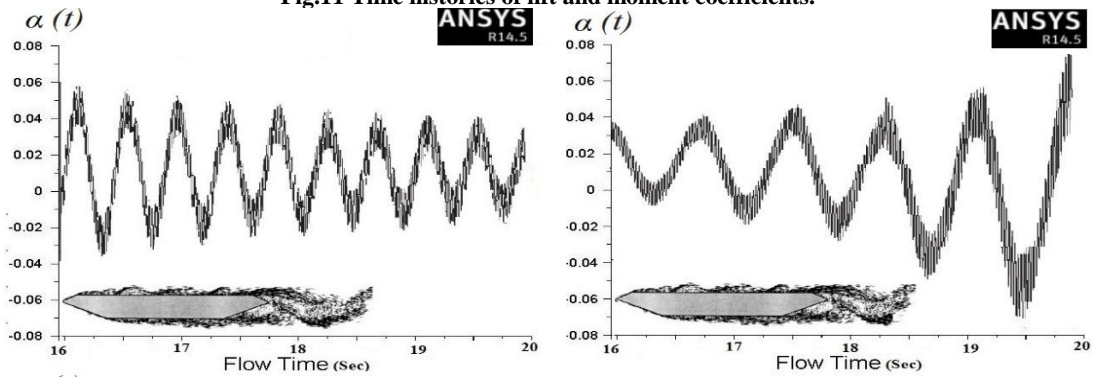


b) V= 69 m/sec



c) V= 70 m/sec

Fig.11 Time histories of lift and moment coefficients.



(a) V=68 m/sec

(b) V=70 m/sec

Fig.12 Time histories of torsional displacement for deck section (1)

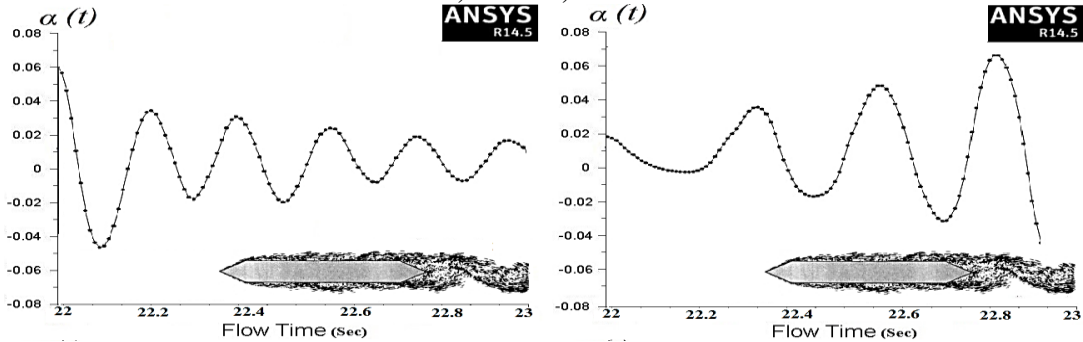


Fig.13 Time histories of torsional displacement for deck section (2).
 (a) V=63 m/sec (b) V=64 m/sec

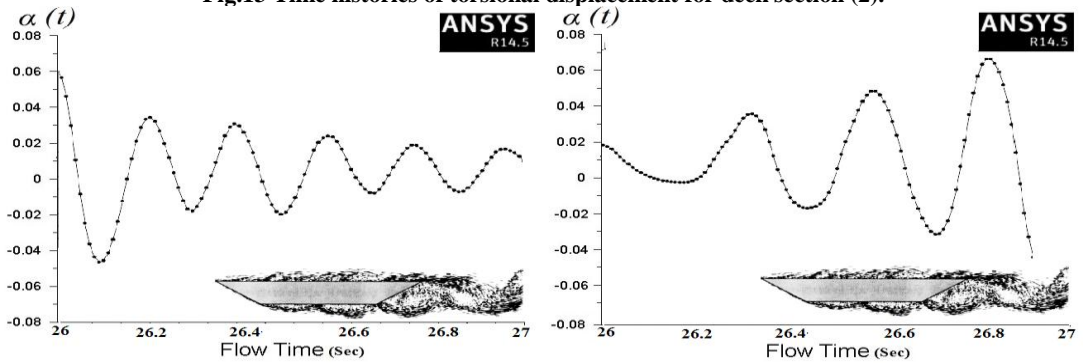


Fig.14 Time histories of torsional displacement for deck section (2).
 (a) V=60 m/sec (b) V=61 m/sec

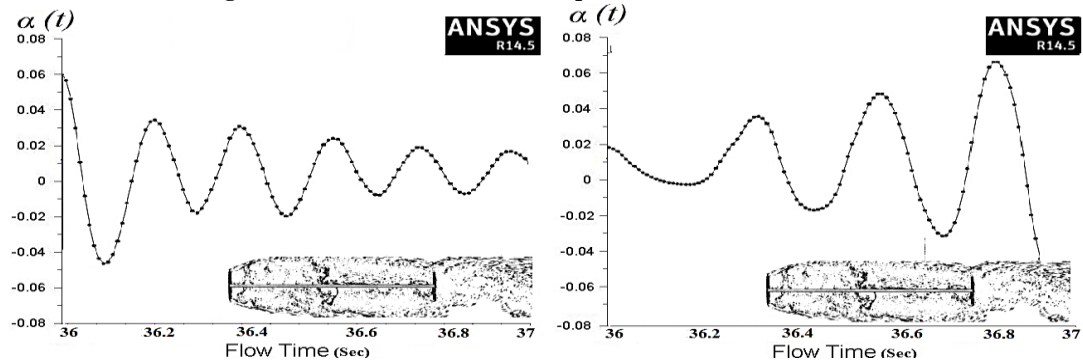


Fig.15 Time histories of torsional displacement for deck section (4).
 (a) V=25 m/sec (b) V=26 m/sec

C. Comparison of Results

Steady simulations of the deck configuration considering Reynolds number equals 2.5×10^5 and range of angles of attack have offered aerodynamic coefficients close to those obtained from wind tunnel tests for the same Reynolds number as shown in Fig.10. The results of work done for deck section 1 is compared with other researchers results as shown in Table 4. The critical flutter velocity predicted in the present work is in a good agreement with the wind tunnel results.

Table 4 References of Flutter velocity for the Great Belt East Bridge.

Reference	Vcr (m/s)
(Numerical) Present work	70
(Numerical) Robert and Kenneth [10]	71.9
(Numerical) Hao Zhan [1]	69
(Wind Tunnel Tests) Hao Zhan [8]	73

D. Improving aerodynamic performance

Since the streamline trapezoidal box girder like deck section 1 has proven that it is the best section in resisting wind flutter, it is widely used in long span bridge design and construction all over the world. To improve the aerodynamic stability performance a guide wing on each side edge of the deck is used as shown in Fig.16.

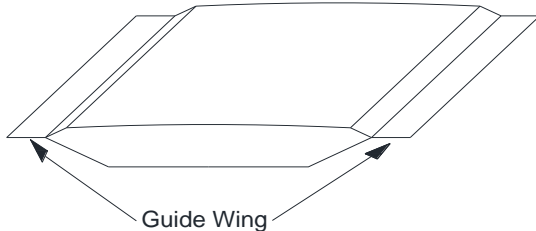


Fig. 16 Outline of guide wing

The guide wing can smooth airflow while passing through the section, hence the aerodynamic stability may be strengthened. It is observed from Table 5 that a wider guide wing can improve the aerodynamic stability distinctly. On the other hand, the complexity of the structure design, construction, and the maintenance cost will be increased.

Table 5 Critical flutter wind speed with guide wings.

Width of Guide Wing (m)	Vcr (m/s)
0.5	71.47
1	72.78
1.5	76.94

IV. CONCLUSIONS

The following points offer the major outcome of the present study:

1. The shape of the bridge deck was a very important cause of failure for the Tacoma Narrows Bridge. There for modern suspension bridges utilize trapezoidal box type sections or sharp leading edges sections like deck sections (1 and 2) and solid girders must be avoided like deck section (4) .
2. The aerodynamics of bridge deck cross sections have been fully described through CFD simulations by using Ansys software.
3. Steady CFD simulation curves of the aerodynamic coefficients have been evaluated for a wide range of angles of attack and the computed results showed acceptable agreement between experimental results and simulation results for the same Reynolds number. Both turbulence models (k-ε) and (k-ω SST) reveled similar results.
4. Unsteady 2D simulations of time history analysis for aerodynamic coefficients led to find the critical wind speed of flutter by increasing the inlet velocity incrementally in different runs. When the aerodynamic coefficient and motion amplitude started growing (negative damping), the critical wind speed was found.

5. The critical velocity for the onset of flutter was predicted successfully and it is in a good agreement with wind tunnel results and work done by other researchers. The obtained critical flutter velocity for deck (1) is 70 m/sec and agrees well with 73 m/s from the wind tunnel measurements.
6. Using a guide wing can smooth airflow while passing through the section and the aerodynamic stability will be strengthened. On the other hand, the guide wing will increase the complexity of the structure design, construction and the maintenance cost.
7. FSI is considered as a direct simulation method for the flutter stability of bridge deck and was developed based on CFD software Fluent and proved to be useful in the early aerodynamic design stage of long span suspension bridges.
8. In the near future fluid-structure interaction (FSI) based on computational fluid dynamics (CFD) will be used in studying complex geometry decks of suspension bridges considering details such as guardrails, cables and aerodynamic appendages. Refinements in processing time and semi-implicit schemes can also be expected.

ACKNOWLEDGEMENT

I am very grateful to Prof.Eman EL-Shamy, Structural Engineering Department, Zagazig University, Egypt for the many valuable comments to the manuscript.

REFERENCES

- [1] Hao Zhan ,Tao Fang ,Zhiguo Zhang.(2013),"Flutter stability studies of Great Belt East suspension bridge by two CFD numerical simulation methods", 6th European & African Conference on Wind Engineering, Robinson College, Cambridge, UK, 7-11 July.
- [2] W.M. Zhang, Y.J. Ge and M.L. Levitan (2011)," Aerodynamic flutter analysis of a new suspension bridge with double main spans", journal of Wind and Structures, **14** (3).
- [3] Vikas Arora. (2015)," Hybrid Viscous-Structural Damping Identification Method" Vibration Engineering and Technology of Machinery, Mechanisms and Machine Science Vol. 23, 2015, pp 209-218.
- [4] Félix Nieto, Ibuki Kusano, Santiago Hernández, José Á. Jurado. (2010)," CFD analysis of the vortex-shedding response of a twin-box deck cable-stayed bridge, The Fifth International Symposium on Computational Wind Engineering Chapel Hill, North Carolina, USA, 23-27 May.
- [5] Xiaobing Liu, Zhengqing ,and Chenb Zhiwen Liu.(2012), "Direct simulation method for flutter stability of bridge deck", The Seventh International Colloquium on Bluff Body Aerodynamics and Applications (BBAA7),Shanghai, China; 2-6 September.
- [6] Gergely Szabó, József Györgyi and Gergely Kristóf. (2012), Advanced flutter simulation of flexible bridge decks, Coupled Systems Mechanics, Vol. 1, No. 2 133-154.
- [7] Ansys Help, Release 14.5 Documentation for Ansys, Fluid Dynamics, Ansys Fluent, Innovative turbulence modeling: in Ansys Fluent, (www.ansys.com).

- [8] Hao Zhan, Tao Fang.(2012), "Flutter stability studies of Great Belt East Bridge and Tacoma Narrows Bridge by CFD numerical simulation", The Seventh International Colloquium on Bluff Body Aerodynamics and Applications (BBAA7) ,Shanghai, China; 2-6 September.
- [9] Ashtiani Abdi, I. (2011) "Experimental and Numerical Investigation of the Wind Effects on Long Span Bridge Decks". Master's thesis, Middle East Technical University, Turkey.
- [10] Robert Stevens and Kenneth Simonsen. (2008), Master's degree in Civil and Structural Engineering at the University of Aalborg.

AUTHOR BIOGRAPHY



First Author: PhD Student in Cairo University and Assistant Lecturer,
Civil Eng. Dept., Higher Technological Institute, 6 October, Egypt
E-mail: Eng_ahmed_abd_elaziz@yahoo.com

Second Author: Professor of theory of Structure, Cairo University, Giza,
Egypt
E-mail: Waattia@gmail.com